Automatic Disturbances Rejection Control-based Model Predictive Torque Control for Permanent Magnet Synchronous Motor with Three-phase Four-switch Inverter

Qing-Fang Teng[1], Guo-Fei Li[1], Jian-Guo Zhu[2], You-Guang Guo[2]

[1]Department of Automation and Electrical Engineering, Lanzhou Jiaotong University, Lanzhou, Gansu, 730070, P.R.C

[2]Faculty of Engineering and Information Technology, University of Technology Sydney, Sydney, NSW, 2007, AUSTRALIA

Abstract: -A novel automatic disturbances rejection control (ADRC)-based Model predictive torque control (MPTC) strategy is developed for permanent magnet synchronous motor (PMSM) with three-phase four-switch inverter. The dynamic model of PMSM with three-phase four-switch inverter is built. The ADRC and MPTC are respectively designed, the former being used to realize disturbance estimation and disturbance compensation while the latter being used to reduce torque and flux ripples. The resultant ADRC-based MPTC PMSM with unhealthy inverter, on the one hand, has fault-tolerant effective and has almost as dynamical performance as ADRC-based MPTC PMSM with healthy inverter, and on the other hand, compared with PI-based MPTC PMSM with unhealthy inverter, it possesses better command-following characteristics and disturbance rejection characteristics in the presence of variations of reference speed and load torque and its total harmonic distortion can be decreased. The simulation results validate the feasibility and effectiveness of the proposed scheme.

Key-words: Model predictive torque control (MPTC); Automatic disturbances rejection control; Fault-tolerant control; Permanent magnet synchronous motor (PMSM); Three-phase four-switch inverter

1 Introduction

The electrical drive systems of modern automotive and aerospace must be required to be high reliable and safe. Due to a variety of complex factors, potential failures are often inevitable. Once the electrical drive is out of order, if repairs and maintenance can not be completed on the spot, this will result in the system to stop working, may cause great financial losses, and even result in enormous human and property losses. Therefore, there is an urgent need to research fault-control for electrical motor.

This work was supported by National Natural Science Foundation of China (No. 61463025)

One of the most common types of potential faults in electrical motor is the loss of one transistor (LOT) in legs of the inverter. If LOT happens suddenly, the corresponding phase is open-circuited, supply and load currents are significantly distorted and the load phase current in which the failure occurred has large zero periods resulting in a loss of torque control and in high pulsating unacceptably torques. Consequently, the drive system's operation has to be interrupted [1, 2]. So it is indispensable to solve the problem such that motor system is designed to be coupled with a fault-tolerant inverter topology and its control strategy is able to manage the drive system during the fault.

Over the past years, mainly three kinds of reconfiguration of inverter topologies for

overcoming inverter faults have been proposed and developed [3, 4]. The first is known as split capacitor scheme for isolating the phase with a faulted inverter leg and connecting the neutral point of the stator windings to the midpoint of DC link [5]. The second is called extra-leg extra-switch scheme by means of connecting the neutral point of the stator windings to an extra inverter leg via an extra switch, which provides the current path during the fault operation [6, 7]. The third is named as extra-leg split capacitor scheme, which adds three TRIACs to connect the midpoint of DC link to three phases of motor, respectively [8-12]. What the first two have in common is that their hardware configuration leaves the electrical machine to operate in a two-phase mode after power device faults, equivalent to the case of disconnection of a motor phase. In contrast, the third inverter topology enables the electrical machine to still operate in a three-phase mode during power device fault, so it is referred to as three-phase four-switch mode. The disadvantage of the first two reconfigurations lies in that a technical solution is required for availability of the neutral point of the stator windings during inverter fault. In order to avoid the above-mentioned disadvantage, the third reconfiguration, i.e. three-phase four-switch mode, is employed in this paper.

Permanent magnet synchronous motor (PMSM) drive nowadays is widely used in the industry applications due to their high efficiency and high power/torque density. As for PMSM drive systems with fault-tolerant inverter, the popular drive control strategies include two types: field oriented control (FOC) and direct torque control (DTC).Making use of FOC strategy, the performance of faulty electric drive systems can be maintained via controlling current [2]. Due to the inherent bandwidth of inner current loop, the dynamic response of FOC drive systems is limited. To improve the dynamic performance, DTC has recently begun to be applied. Compared to FOC, DTC directly manipulates the inverter's output voltage vector, hence eliminates the inherent delay caused by current loops and features comparatively fast dynamic response. Even so, switching-table-based DTC presents some unavoidable drawbacks, such as high torque and flux ripples, variable switching frequency along with acoustic noise.

Apart from FOC and DTC, model predictive torque control (MPTC) is an emerging control concept and is received significant attention from electrical drives community [13-17], which adopts the principle of model predictive control (MPC). MPC has several merits such as easy inclusion of nonlinearities and constraints. Besides, its algorithm is simple and then its implementation is easy. Compared with two state-of-the art schemes above-mentioned, MPTC achieves faster response than FOC and more obvious reduction of the torque and flux ripples than DTC. Furthermore, switching losses can be reduced. Even so, a little work in the past has focused on applying MPTC to PMSM system with fault inverter. It is the abovementioned advantage of MPTC that motivates this paper.

So far, the conventional MPTC PMSM system consists of two loops, one being outer-loop and the other being inner-loop. In general, PI and MPTC are acted as outer-loop and inner-loop, respectively. For the PI-based MPTC PMSM systems, PI is to regulate the rotor speed and generate the reference torque and its parameters commonly adopt a fixed gain. They may perform well under certain operating conditions, but degrade dynamic performance under other operating conditions when external disturbances and internal perturbations arise. For more than decade, many researchers have contributed their efforts toward strong-robustness control of PMSM motors, and various algorithms have been proposed. Among them, automatic disturbances rejection control (ADRC), firstly

proposed by Han [18], has been proved to be unmistakable advantage in performance and practicality [19, 20]. ADRC inherits the quality from PID and meanwhile conquers PID's weakness. The key of ADRC is to reformulate the problem by lumping various known and unknown quantities that affect the system performance into total disturbance [21]. And the total disturbance can be actively estimated and then rejected. For this reason, we propose replacement of PI with ADRC in our research.

For three-phase four-switch inverter in PMSM drive systems, in order to improve dynamic performance and system robustness, a novel ADRC-based MPTC strategy is proposed in our research.

The structure of the paper is as follows: modeling of PMSM with three-phase four-switch inverter is given in section two. In section three, the ADRC-based MPTC PMSM system is established, and the ADRC and MPTC are designed, respectively. The numerical simulation result & analysis and conclusion are reported in section four and five, respectively.

2 Dynamic model of PMSM with three-phase four-switch inverter

In this paper, as for three-phase PMSM, the schematic diagram of fault-tolerant three-phase four-switch inverter topology is shown in Fig. 1.

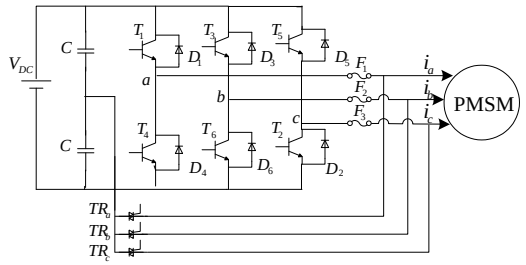

Fig.1 Fault-tolerant inverter topology

We suppose one transistor to be off on inverter leg corresponding phase *a*. Then the series-connected fuse F_1 is disconnected and the corresponding TRa is triggered. So the faulted inverter leg is isolated and replaced by extra-leg split capacitor. Fig.1 can be changed into three-phase four-switch inverter as shown in Fig.2.

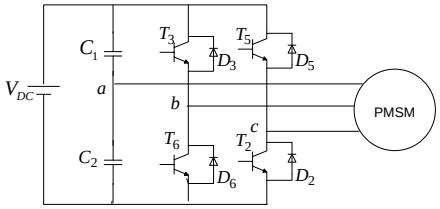

Fig.2 Three-phase four-switch inverter and PMSM drive

As for Fig.2, three-phase stator voltages in *abc*-system are given by:

$$\begin{cases} u_a = V_{DC}(1 - S_b - S_c)/3 \\ u_b = V_{DC}(-1/2 + 2S_b - S_c)/3 \\ u_c = V_{DC}(-1/2 - S_b + 2S_c)/3 \end{cases} \quad (1)$$

Where u_a, u_b and u_c are stator voltages in *abc*-system, V_{DC} is DC bus voltage of power unit, S_i (i= b, c) is upper power switch state of one of two legs. S_i =1 or S_i =0 when upper power switch is on or off as shown in Fig.2. The different combination of S_b, S_c may form four switching states, which produce corresponding four voltage space vectors V_1-V_4 as shown in Fig. 3. Obviously, the magnitudes of four voltage space vectors are not equal.

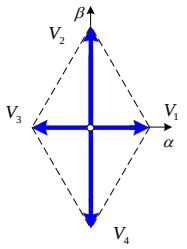

Fig.3 The layout of voltage space vectors of three-phase four-switch inverter

Consider surface-mounted PMSM, the model in $\alpha\beta$ -system is expressed as follows

$$\begin{cases} \dot{i}_\alpha = \left(-R_s i_\alpha + \psi_f \omega_r \sin(p\theta_r) + u_\alpha\right)/L \\ \dot{i}_\beta = \left(-R_s i_\beta - \psi_f \omega_r \cos(p\theta_r) + u_\beta\right)/L \end{cases} \quad (2)$$

$$\begin{cases} \dot{\psi}_\alpha = u_\alpha - R_s i_\alpha \\ \dot{\psi}_\beta = u_\beta - R_s i_\beta \end{cases} \quad (3)$$

Where i_α, i_β, u_α, u_β, ψ_α, ψ_β are α -axis and β -axis stator currents, voltage, flux, respectively, in $\alpha\beta$ -system. L stator-winding inductance, R_s stator resistance. ψ_f permanent magnet flux. ω_r, θ_r stand, respectively, for the measured angular rotor displacement and the angular speed.

And the electromagnetic torque is expressed as

$$J\dot{\omega}_r = T_e - T_l - B_m\omega_r - T_f \qquad (4)$$

Where J, T_e , T_l , B_m and T_f are respectively inertia of moment, electromagnetic torque, exogenous load torque, viscous friction coefficient and coulomb friction torque. p the number of pole pairs.

3 Design of ADRC-based MPTC for PMSM systems with three-phase four-switch inverter

The objective of ADRC-based MPTC for PMSM drive system with three-phase four-switch is that the drive system not only can work reliably and its speed & torque can be controlled to achieve satisfactory dynamic performance but also can be strong robust to motor parameter variation and external disturbance. The control diagram of ADRC-based MPTC system proposed is shown in Fig.4.

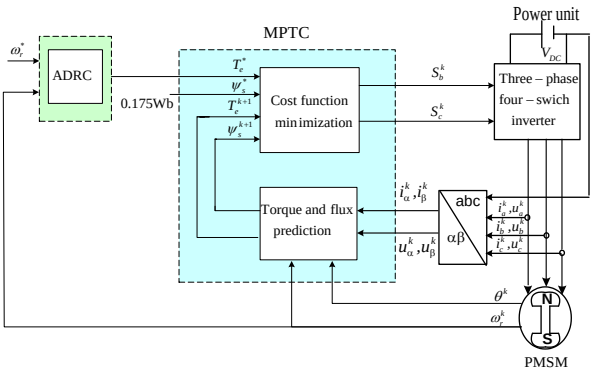

Fig.4 ADRC-based MPTC for PMSM with three-phase four-switch inverter

It mainly comprises of three components: ADRC, MPTC, power unit. MPTC includes two parts: cost function minimization and torque & flux prediction as shown in Fig. 4. And power unit employs three-phase four-switch inverter.

3.1 ADRC design

The schematic diagram of ADRC is shown in Fig. 5, which consists of an extended state observer (ESO) and a nonlinear function (NF). The ESO is used to estimate the unmeasured state and the real action of the unknown disturbances to build a solid base for better performance and disturbances compensation. The NF is used to synthesize the control action.

3.1.1 ESO design

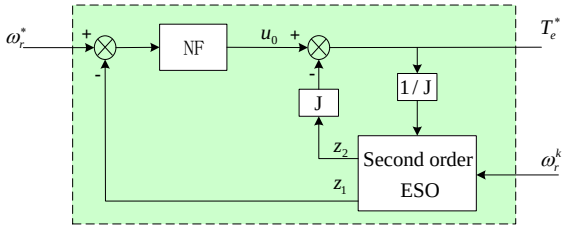

Fig.5 Schematic diagram of ADRC

Let $x_1 = \omega_r$, (5)

The state space equation of (4) is yielded as following

$$\dot{x}_1 = -B_m x_1/J - \left(T_l + T_f\right)\Big/J + T_e/J \qquad (6)$$

where T_e can be seen as the control input.

From (4), it can be seen that the variation of load torque, inertia of moment and viscous friction have negative effects on dynamic performance of PMSM system. So the negative effects can be viewed as the disturbance which is marked by *f(t)*. According to ADRC principle, *f(t)* is defined as

$$f(t) = -B_m\omega_r/J - \left(T_l + T_f\right)\Big/J \qquad (7)$$

From (7), it can be observed that *f(t)* is a multivariable function of both the state and external disturbances as well as time and thus can be regarded as the total disturbance. The objective here is to overcome the total disturbance by the control input T_e and to make x_1 behave as desired value. At this point, our crucial task is to identify and reject the total disturbance *f(t)*.

Treating *f(t)* as an augmented variable $x_2 = f(t)$, and let $\dot{f}(t) = g(t)$, with $g(t)$ unknown, the original plant in (6) is rewritten as

$$\begin{cases} \dot{x}_1 = x_2 + T_e/J \\ \dot{x}_2 = g(t) \end{cases} \qquad (8)$$

which is observable. Now we construct a

second-order state observer, denoted as the ESO, in the form of

$$\begin{cases} e = \omega_r - z_1 \\ \dot{z}_1 = z_2 - \beta_1 fal(e, a_1, \delta_1) + T_e / J \\ \dot{z}_2 = -\beta_2 fal(e, a_2, \delta_2) \end{cases} \quad (9)$$

where β_1 and β_2 are positive observer gains, a_1, a_2 and δ_1 are positive parameters, $fal(x,a,\delta)$ is a nonlinear function which is defined as

$$fal(x,a,\delta) = \begin{cases} x/\delta^{1-a}, & |x| \le \delta \\ \text{sign}(x) \cdot |x|^a, & |x| > \delta \end{cases} \quad (10)$$

***Remark* 1:** The input to ESO are the reference torque T_e^* and measured rotor speed ω_r, and the output of ESO identifies the important information *f(t)*.

Remark* 2*: As far as the above-mentioned parameters of ESO, generally, $0 < a_i \le 1$ and δ_i $(i = 1,2)$ can be selected from the range of [0.0001 1], and small δ_i is helpful for the noise suppression. $\beta_i (i = 1,2)$ can be determined based on the tracking performance, and large β_i is helpful to improve the tracking speed. There is a tradeoff between δ_i and β_i for a better noise suppression and tracking performance.

3.1.2Disturbance Rejection

Once observer (9) is well tuned, its output will track x_1 and *f(t)*, respectively. By canceling the influence of total disturbance *f(t)* using z_2, ADRC actively compensates for *f(t)* in real time. The controller is designed as [22]

$$T_e^* = u_0(t) - Jz_2 \quad (11)$$

where $u_0(t)$ is output of NF defined as

$$u_0(t) = \beta_3 fal(\omega_r^* - z_1, a_3, \delta_3) \quad (12)$$

3.2Model predictive torque control

3.2.1 Basic principle of MPTC

The basic idea of MPTC is to predict the future behavior of the variables over a time frame based on the model of the system. In fact, MPTC is an extension of DTC, as it replaces the look-up table of DTC with an online optimization process in the control of machine torque and flux. Different from the employments of hysteresis comparators and switching table in DTC, the principle of vector selection in MPTC is based on evaluating a defined cost function. The selected voltage vector from switching table in DTC is not necessarily the best one in terms of reducing torque and flux ripples. For four voltage space vectors generated by three-phase four-switch inverter as shown in Fig.3, it is easy to evaluate the effect of each voltage vector and select the one to minimize the cost function in MPTC.

For conventional MPTC, the minimum cost function is such chosen that both torque and flux at the end of the cycle are as close as possible to their reference values. Its definition is as follows

$$\begin{aligned} &\min.\{g_i\} = \left|T_e^* - T_e^{k+1}\right| + k_1 \left|\left|\psi_s^*\right| - \left|\psi_s^{k+1}\right|\right| \\ &s.t. V_i \in \{V_1 \quad V_2 \quad V_3 \quad V_4\}, i = 1, \cdots, 4 \end{aligned} \quad (13)$$

where T_e^* and ψ_s^* are reference values for torque and stator flux, respectively. T_e^{k+1} and ψ_s^{k+1} predictions for torque and stator flux at (k+1)th instant, respectively. k_1 is the weighting factor. V_1, V_2, V_3, and V_4 as shown in Fig. 3 are generated by three-phase four-switch inverter with respect to the different switches states.

3.2.2 Predictive model for stator currents

According to (2), the prediction of the stator currents at (k+1)th instant is expressed as

$$\begin{cases} i_\alpha^{k+1} = i_\alpha^k + \left(-R_s i_\alpha^k + \psi_f \omega_r^k \sin p\theta_r^k + u_\alpha^k\right) T_s / L \\ i_\beta^{k+1} = i_\beta^k + \left(-R_s i_\beta^k - \psi_f \omega_r^k \cos p\theta_r^k + u_\beta^k\right) T_s / L \end{cases} \quad (14)$$

where i_α^{k+1} and i_β^{k+1} are predicted values of stator currents at (k+1)th instant, T_s is the sampling period.

After obtaining i_α^{k+1} and i_β^{k+1}, both the torque and flux at the (k+1)th instant can be estimated according to the following section

3.2.3.

3.2.3 Torque and flux estimators

According to (3), the predictions of the flux-linkage at the (k+1)th instant can be expressed as following:

$$\begin{cases} \psi_\alpha^{k+1} = \psi_\alpha^k + T_s(u_\alpha^k - R_s i_\alpha^k) \\ \psi_\beta^{k+1} = \psi_\beta^k + T_s(u_\beta^k - R_s i_\beta^k) \end{cases} \quad (15)$$

The predictions of the magnitudes of stator flux linkage and electromagnetic torque at the (k+1)*th* instant respectively are

$$\psi_s^{k+1} = \sqrt{\left(\psi_\alpha^{k+1}\right)^2 + \left(\psi_\beta^{k+1}\right)^2} \quad (16)$$

$$T_e^{k+1} = 1.5p\left(\psi_\alpha^{k+1} i_\beta^{k+1} - \psi_\beta^{k+1} i_\alpha^{k+1}\right) \quad (17)$$

Substituting (14) and (15) into (17), the predictive torque can be estimated.

4 Simulation and analysis

In order to validate the effective of proposed control scheme, the designed control system from Fig.4 has been implemented in Matlab/Simulink/Simscape platform. The parameters of PMSM: R_s is 2.875 Ω, L is 0.0085H, ψ_f is 0.175Wb, p is 1, V_{dc} is 350V, n_N is 3000rpm, J is 0.0008Kg.m^2, T_n is 3N.m, T_f is 0 and B_m is 0.001Nms. The sampling period T_s is 10 μ s, and value k_1 in (13) is selected to be 33. The parameters of ADRC in Fig.4 are determined as follows,

$$a_1 = a_2 = a_3 = 0.5, \quad \delta_1 = \delta_2 = \delta_3 = 0.01$$
$$\beta_1 = 750, \quad \beta_2 = 6000, \quad \beta_3 = 16$$

The following two groups of simulations were carried out. The first concerned the fault-tolerant effect of ADRC-based MPTC for PMSM with unhealthy inverter. The second concerned the robustness of the proposed scheme to disturbance.

4.1 Fault-tolerant effect

In order to validate the fault-tolerant effective of proposed scheme, two systems were compared, one corresponding to the PMSM with healthy inverter, i.e. three-phase six-switch inverter, and the other corresponding to the PMSM with unhealthy inverter, i.e. three-phase four-switch inverter. Except the above-mentioned distinct inverters, two systems had completely the same structure and parameters of ADRC-based MPTC strategy.

Figs.6 and 7 show their comparison results in terms of rotor speed, torque and stator currents when the reference speed n^* is set to 1000 rpm, the load torque of 1N.m. Comparing Fig.6 with Fig.7, it can be seen that, for the PMSM system with unhealthy inverter, it had fault-tolerant effective and its speed and torque could be regulated in a satisfactory manner and had almost as good performance as the PMSM system with healthy inverter.

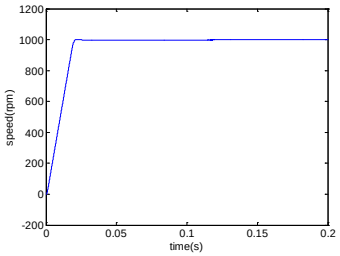

(a) Rotor speed response

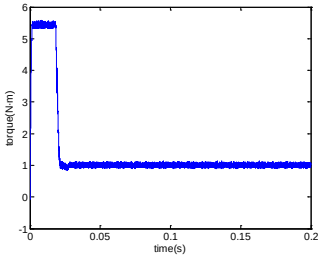

(b) Torque response

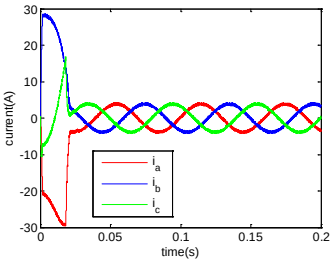

(c) Stator currents i_a, i_b and i_c

Fig.6 Dynamic responses for PMSM with healthy inverter

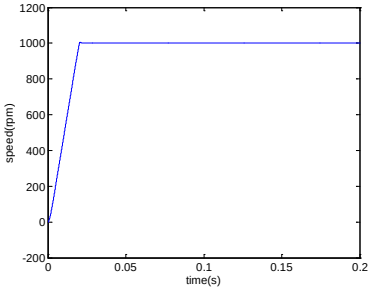

(a) Rotor speed response

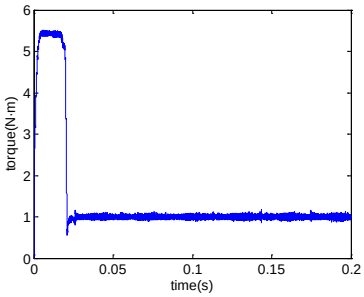

(b) Torque response

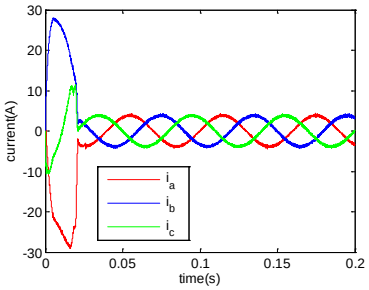

(c) Stator currents i_a,i_b and i_c

Fig.7 Dynamic responses for PMSM with unhealthy inverter

4.2 Robustness

For the ADRC-based MPTC PMSM systems with unhealthy inverter, for the sake of verifying its stronger robustness, two systems of simulations were compared, which correspond to the PI-based MPTC and ADRC-based MPTC PMSM systems, respectively. Except distinct outer-loop controllers (i.e. PI and ADRC), two systems had completely the same structure and parameters of MPTC.

4.2.1 Performance comparison under the variation of load torque

The parameters of PI for PI-based MPTC PMSM system are adjusted as follows,

$$K_p = 0.16, K_I = 0.1$$

such that PI-based MPTC system has the same transient response as ADRC-based one.

In the simulation, their reference speeds n^* are set to 1000 rpm and their load torques of 1N.m are increased to 2 Nm at 0.2s.

Figs.8 and 9 show their dynamical responses. Comparing Fig.8(a) with Fig.9(a), it can be seen that, for ADRC-based MPTC PMSM system, its speed can sharply adapt to the change of external load change in a satisfactory manner, and its capable of accommodating the challenge of load disturbance is superior to PI-based one's.

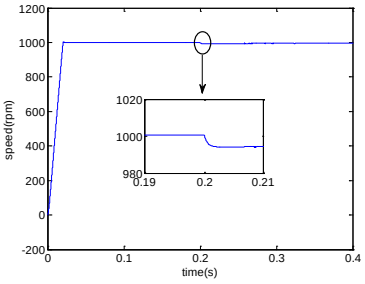

(a) Rotor speed response

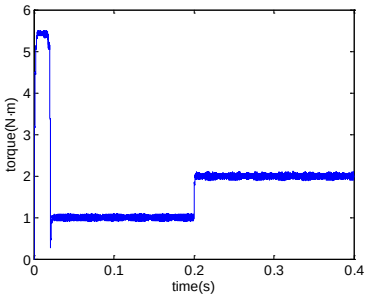

(b) Torque response

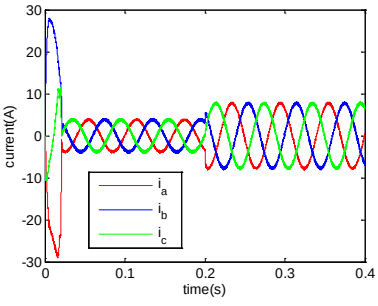

(c) Stator currents i_a,i_b and i_c

Fig.8 Dynamic responses of PI-based MPTC scheme for PMSM with unhealthy inverter

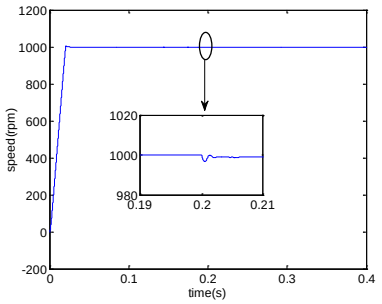

(*a*) Rotor speed response

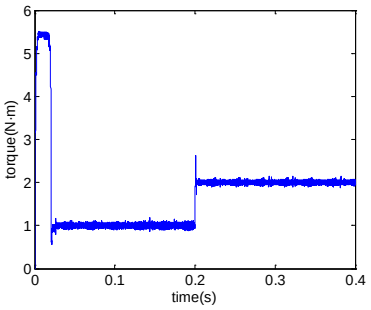

(*b*) Torque response

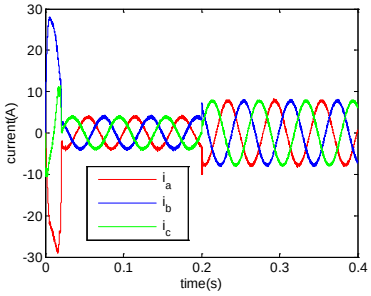

(c) Stator currents i_a,i_b and i_c

Fig.9 Dynamic responses of ADRC-based MPTC scheme for PMSM with unhealthy inverter

4.2.2 Performance comparison under the variation of reference speed

The parameters of PI are determined as follows,

$$K_p = 1.5, K_I = 0.01$$

such that PI-based MPTC system has the same anti-load disturbance as ADRC-based one.

In the simulation, their reference speeds n^* of 800 rpm are increased to 1000 rpm at 0.1s and then decreased to 600rpm at 0.3s, their load torques of 1N.m are increased to 2 Nm at 0.2s.

1）Dynamical response comparison

Fig. 10 and 11 show their dynamical responses in terms of torque and stator currents. Fig.12 intuitively gives their speed response comparison. From these simulation results, it can be observed that, for the PMSM with unhealthy inverter, the ADRC-based MPTC has smaller overshoot and faster settling time than PI-based one.

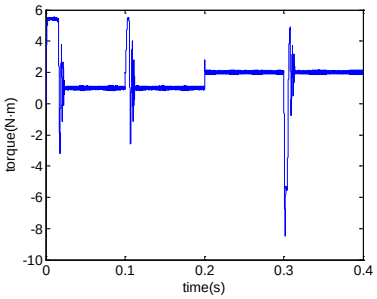

(a) Torque response

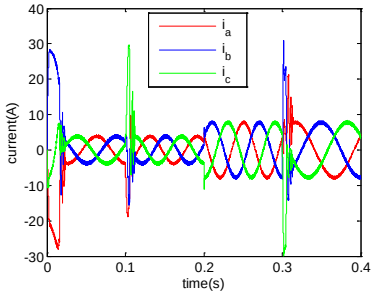

(b) Stator currents i_a,i_b and i_c

Fig.10 Dynamic responses of PI-based MPTC scheme for PMSM with unhealthy inverter

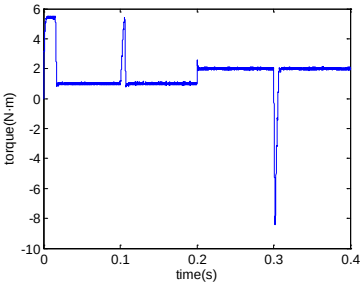

(a) Torque response

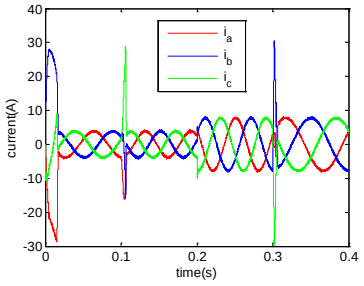

(b) Stator currents i_a,i_b and i_c

Fig.11 Dynamic responses of ADRC-based MPTC scheme for PMSM with unhealthy inverter

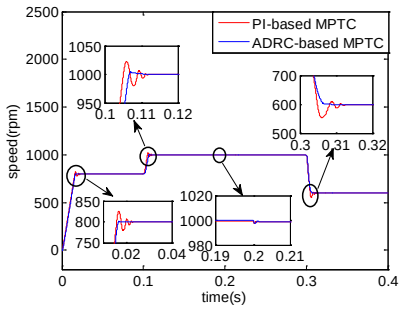

Fig.12 Speed response comparison between PI-based and ADRC-based MPTC schemes for PMSM with unhealthy inverter

2）THD comparison of the phase current

Given that the three-phase currents measurements are recorded over the time range from 0.2s to 0.3s. During this time range, the fundamental frequency of three-phase currents is 16.67 Hz. THD can be obtained by comparing the higher frequency components to the fundamental one of the three-phase stator currents.

Table 1 shows THD comparison of three-phase currents for PI-based and ADRC-based MPTC PMSM systems. From table 1, what can be observed is that the ADRC-based MPTC strategy decreases the THD as opposed to PI-based MPTC one.

TABLE 1 THD OF THREE-PHASE STATOR CURRENTS

Control scheme	i_a	i_b	i_c
PI-based MPTC	1.90%	2.87%	2.90%
ADRC-based MPTC	1.35%	1.63%	1.52%

From these experiments, it can be summarized that, compared with PI-based MPTC PMSM with unhealthy inverter, ADRC-based one can achieve more satisfactory dynamic behavior and smaller THD value.

5 Conclusion

In this paper, ADRC-based MPTC strategy has been developed for PMSM with three-phase four-switch inverter. The mathematical model of PMSM with fault-tolerant inverter topology is built. The ADRC and MPTC are designed, respectively, ADRC being to realize disturbance estimation and disturbance compensation and MPTC being to reduce torque & flux ripples. The resultant ADRC-based MPTC for PMSM with three-phase four-switch inverter has fault-tolerant effective and its speed and torque could be regulated in a satisfactory manner and have almost as performance as the PMSM system with healthy inverter. Compared with PI-based MPTC PMSM with unhealthy inverter, ADRC-based one possesses the better command-following characteristics and disturbance rejection characteristics in the presence of variation of reference speed and load torque, and its THD can be decreased. The proposed ADRC-based MPTC PMSM with unhealthy inverter achieves satisfactory dynamical performance and strong robustness. Comparative simulations demonstrate the feasibility and effectiveness of the proposed scheme.

References

[1] P. Potamianos, E. Mitronikas and A. Safacas, A Fault Tolerant Modulation Strategy for Matrix Converters, *5th IET International Conference on Power Electronics*, Machines and Drives (PEMD 2010), pp.1-6,2010.

[2] T. H. Liu, J. R. Fu and T. A. Lipo, A Strategy for Improving Reliability of Field-Oriented Controlled Induction Motor Drives, *IEEE Transactions on Industry Applications*, Vol. 29, No. 5, pp.910-918, 1993.

[3] Behrooz M. Survey of fault-tolerance techniques for three-phase voltage source inverters. *IEEE Transactions on Industrial Electronics*, Vol. 61, No. 10, pp.5192-5202, 2014.

[4] Q. T. An. Diagnosis and fault tolerant control strategies of inverters in three-phase motor drive systems, Ph.D. dissertation, Harbin Institute of Technology, China, 2011.

[5] Gaeta A, Scelba G, Consoli A. Modeling and control of three-phase PMSMs under open-phase fault. *IEEE Transactions on*

Industry Applications, Vol. 49, No. 1, pp.74-83, 2013.

[6] Hoang K D, Zhu Z Q, Foster M. Direct torque control of permanent magnet brushless AC drive with single-phase open-circuit fault accounting for influence of inverter voltage drop. *IET Electric Power Applications*, Vol. 7, No. 5, pp.369-380, 2013.

[7] Q.F. Teng, J.G. Zhu, T.S. Wang and G. Lei, "Fault Tolerant Direct Torque Control of Three-Phase Permanent Magnet Synchronous Motors," *WSEAS Transactions on systems*, vol.11, no.11, pp.465-476, 2012.

[8] K. Zhao, Q. T. An, L. Sun, W. Ye. Fault-tolerant inverter permanent synchronous motor position sensorless control system. *Electric machine and control*, vol.14, no.4, pp.25-30, 2012.

[9] Campos-Delgado D U, Espinoza-Trejo D R, Palacios E. Fault-tolerant control in variable speed drives: a survey.*IET Electric Power Applications*, vol.2, no.2, pp.121-134, 2008.

[10] Mendes A M S, Cardoso A J M. Fault-tolerant operating strategies applied to three-phase induction-motor drives. *IEEE Transactions on Industrial Electronics*, vol.53, no.6, pp.1807-1817, 2006.

[11] D. Sun, Y. K. He, Z. Y. He. Fault tolerant inverter based direct torque control for permanent magnet synchronous motor. *Journal of Zhejiang University*, vol.41, no.7, pp.1101-1106, 2007.

[12] Welchko B A, Lipo T A, Jahns T M, et al. Fault tolerant three-phase AC motor drive topologies: a comparison of features, cost, and limitations. *IEEE Transactions on Power Electronics*, vol.19, no.4, pp.1108-1116, 2004.

[13] Geyer T, Papafotiou G, Morari M. Model predictive direct torque control—Part I: Concept, algorithm, and analysis. *IEEE Transactions on Industrial Electronics*, vol.56, no.6, pp.1894-1905, 2009.

[14] Preindl M, Bolognani S. Model predictive direct torque control with finite control set for PMSM drive systems, Part 1: Maximum torque per ampere operation. *IEEE Transactions on Industrial Informatics*, vol.9, no.4, pp.1912-1921, 2013.

[15] Rojas C A, Rodriguez J, Villarroel F, et al. Predictive torque and flux control without weighting factors. *IEEE Transactions on Industrial Electronics*, vol.60, no.2, pp.681-690, 2013.

[16] Wang F, Zhang Z, Alireza D. An experimental assessment of finite-state predictive Torque control for electrical drives by considering different online optimization methods. *Control Engineering Practice*, vol.31, pp.1-8, 2014.

[17] Q. F. Teng, J. Y. Bai, and J. G. Zhu, "Fault Tolerant Model Predictive Control of Three-Phase Permanent Magnet Synchronous Motors," *WSEAS Transactions on systems*, vol.8, no.12, pp.385-397, 2013.

[18] J. Q. Han, Auto Disturbances Rejection Control Technique. *Frontier Science*, no.1, pp.24-31, 2007.

[19] D Sun. Comments on active disturbance rejection control. *IEEE Transactions on Industrial Electronics*, vo54, no.6, pp.3428-3429, 2007.

[20] Hebertt Sira-Ramírez, Jesús Linares-Flores, Carlos García-Rodríguez, et al. On the control of the permanent magnet synchronous motor: an active disturbance rejection control approach. *IEEE Transactions on System Technology*, vo22, no.5, pp.2056-2063, 2014.

[21] J. Q. Han. From PID to active disturbance rejection control. *IEEE transactions on Industrial Electronics*, vo56, no.3, pp.900-906, 2009.

[22] Y. P. Liu. Space vector modulated direct torque control for PMSM based on ADRC. *Electrical Power Automation Equipment*, vo31, no.11, pp.78-82, 2011.